Analysis of deuteron elastic scattering from ^{6,7}Li using the continuum discretized coupled channels method

Tao Ye and Yukinobu Watanabe*
Department of Advanced Energy Engineering Science, Kyushu University, Fukuoka 816-8580, Japan

Kazuyuki Ogata
Department of Physics, Kyushu University, Fukuoka 812-8581, Japan

Satoshi Chiba
Advanced Science Research Center, Japan Atomic Energy Agency, Tokai, Naka, Ibaraki 319-1195, Japan
(Received 16 June 2008; published 29 August 2008)

The continuum discretized coupled channels (CDCC) approach is applied to analysis of deuteron elastic scattering from ^{6,7}Li in the energy range from 10 to 50 MeV. Phenomenological neutron and proton optical potentials that are essentially important in the CDCC calculation are determined from the present optical model analysis of differential cross sections of nucleon elastic scattering, neutron total cross sections, and reaction cross sections of ^{6,7}Li for energies from 5 to 50 MeV. The CDCC result provides satisfactory agreement with experimental data, particularly at forward angles. The obtained nucleon optical model potentials are found to describe reasonably well both nucleon and deuteron elastic scattering from ^{6,7}Li for energies up to 50 MeV.

DOI: 10.1103/PhysRevC.78.024611 PACS number(s): 25.45.De, 25.40.−h, 24.10.Eq, 24.10.Ht

I. INTRODUCTION

Recently, the study of deuteron-induced reactions has attracted interest in association with various neutron applications, since they have a capability of producing high-intensity neutrons. One of the applications is for neutron irradiation testing of fusion reactor candidate materials. For this purpose, an accelerator-driven d-Li neutron source has been proposed as a high-intensity neutron source in the International Fusion Material Irradiation Facility (IFMIF) [1]. In the plan, it is expected that neutrons up to about 55 MeV will be produced by two 125-mA beams of 40-MeV deuterons bombarding a thick target of flowing liquid lithium. Knowledge of the nuclear interaction of deuterons with materials is indispensable for estimating neutron yields and induced radioactivities in the engineering design of such neutron sources and accelerator shielding. From this point of view, reliable nuclear data of deuteron-induced reactions on various nuclei are currently required.

In connection with the IFMIF project, it is of interest to understand the mechanism of deuteron-induced reactions on Li up to 50 MeV. Neutron production from deuteron bombardment with Li occurs via various reaction processes (e.g., deuteron breakup and proton stripping processes, sequential neutron emission from highly excited compound and residual nuclei, and so on). Neutron spectra observed at forward angles show a distinct broad peak at approximately half the incident energy [2]. This suggests the importance of deuteron breakup processes, namely, deuteron dissociation in nuclear fields and proton stripping, which are expected to contribute to major neutron production. In the past works [3,4], these processes in the d + Li reaction were treated by using semiclassical models such as the modified INC model [3] and the Serber model [5]. Since the incident energy of interest here is relatively low, more sophisticated quantum mechanical approaches will be suitable to enhance our understanding of the Li(d, xn) reaction.

We propose to apply the continuum discretized coupled channels (CDCC) method, one of the quantum mechanical approaches, to analyses of the interaction of the deuteron with ^{6,7}Li. The CDCC method [6–9] can deal with the deuteron breakup processes explicitly using a phenomenological three-body Hamiltonian in which the nucleon-nucleus interaction is represented by the optical model potential (OMP) at half the deuteron incident energy and an effective nucleon-nucleon potential is used for the p-n interaction. Recently, the CDCC approach has been widely used as an advanced theoretical tool in the analyses of projectile breakup of exotic and halo nuclei [10,11]. Moreover, the CDCC calculation has been applied successfully to the (d, n) reaction with ^{7}Be, which is a mirror nucleus of ^{7}Li, at 8 MeV [8]. Thus, the CDCC method is expected to be a promising approach to describe the Li(d, xn) reaction well.

In the present work, we analyze deuteron elastic scattering and reaction cross sections for ^{6,7}Li by means of the CDCC method as a first step before applying it to the study of deuteron breakup processes in the Li(d, xn) reaction. Recently, Chau Huu-Tai [12] presented a systematic CDCC analysis of deuteron elastic scattering and reaction cross sections for target nuclei ranging from ^{16}O to ^{208}Pb in the incident energy range from 3 to 200 MeV. His work shows that the global nucleon OMP [13] can be applied satisfactorily well to the CDCC calculation. The nucleon OMP is the most essential ingredient in the CDCC calculation of deuteron-induced reactions. Since ^{6,7}Li nuclei are beyond the mass number range allowed by the global nucleon OMP [13], a preliminary calculation was performed by using two representative global nucleon OMPs for $1p$ shell nuclei [14,15]. However, the result did not

*watanabe@aees.kyushu-u.ac.jp

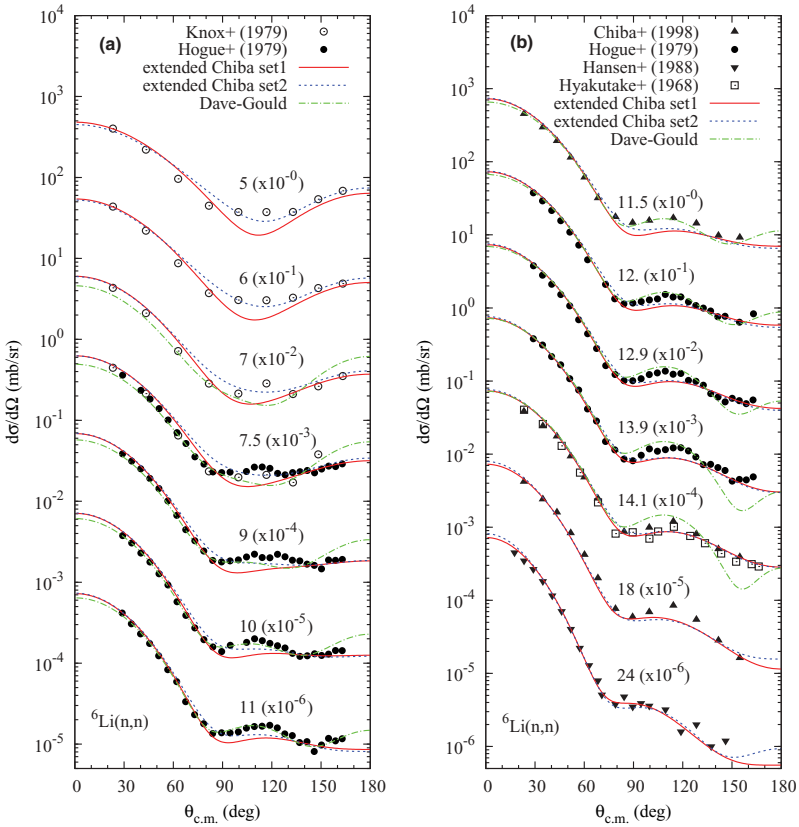

FIG. 1. (Color online) Comparison of the experimental and calculated differential cross sections of neutron elastic scattering from ^{6}Li. The solid and short-dashed curves represent the calculations using the extended Chiba OMP with the Set 1 and Set 2 parameters, respectively. The dash-dotted curves are the results of the Dave-Gould OMP. The number at the top of each plot denotes incident energy in MeV.

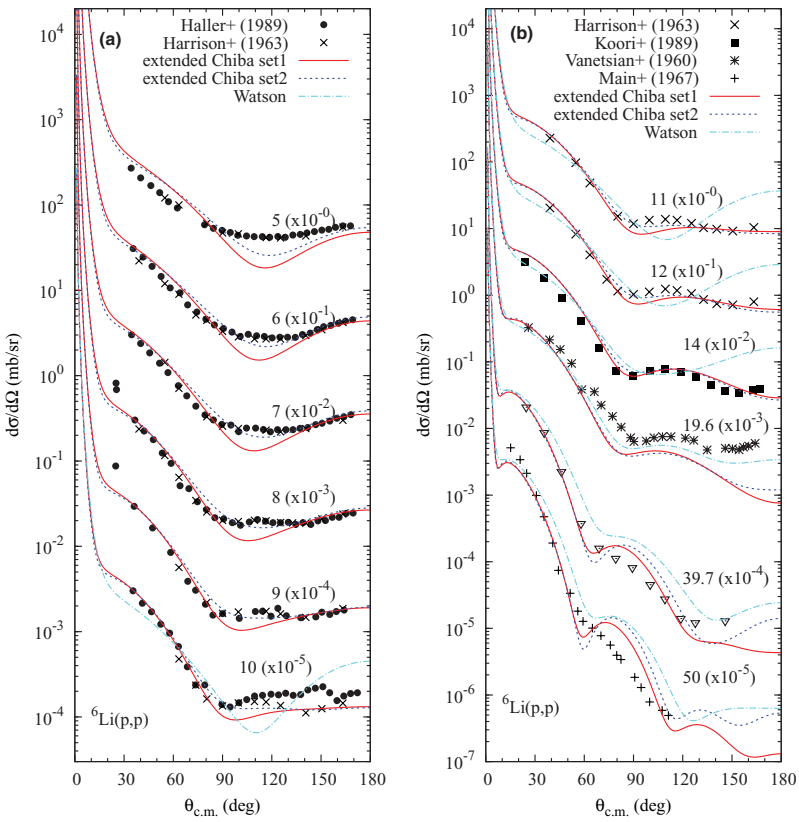

FIG. 2. (Color online) Comparison of experimental and calculated differential cross sections of proton elastic scattering from ^{6}Li. The solid and short-dashed curves represent the calculations using the extended Chiba OMP with the Set 1 and Set 2 parameters, respectively. The dash-dotted curves are the results of the Watson OMP. The number at the top of each plot denotes incident energy in MeV.

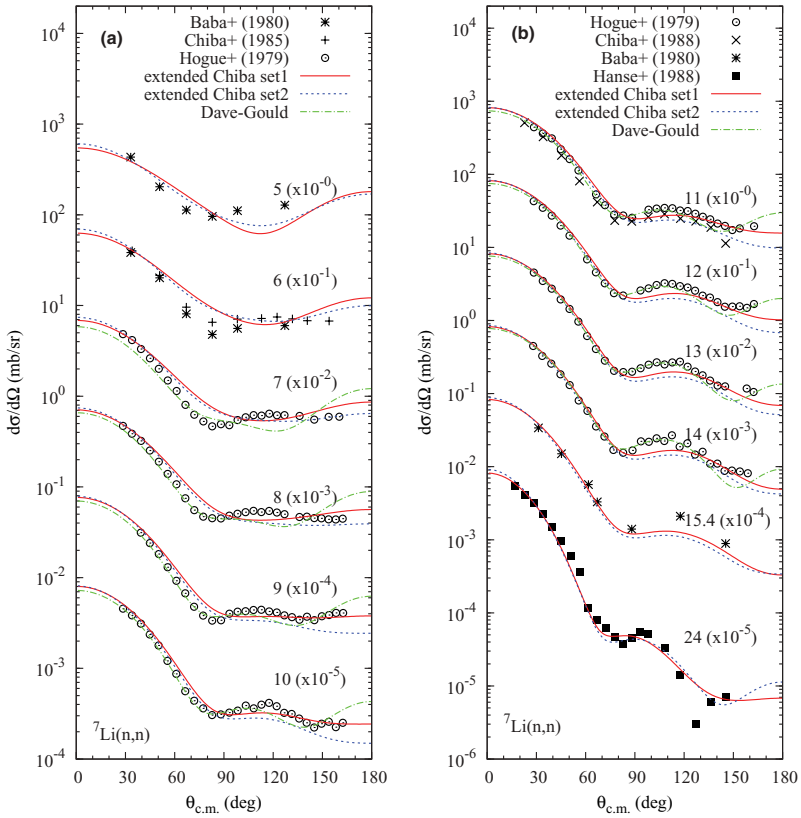

FIG. 3. (Color online) The same as in Fig. 1 but for the target nucleus ^{7}Li. The contribution of inelastic scattering to the excited state (E_{ex} = 0.478 MeV) is included in all the calculations except at 24 MeV. The inelastic cross sections are taken from the JENDL-3.3 nuclear data library [22].

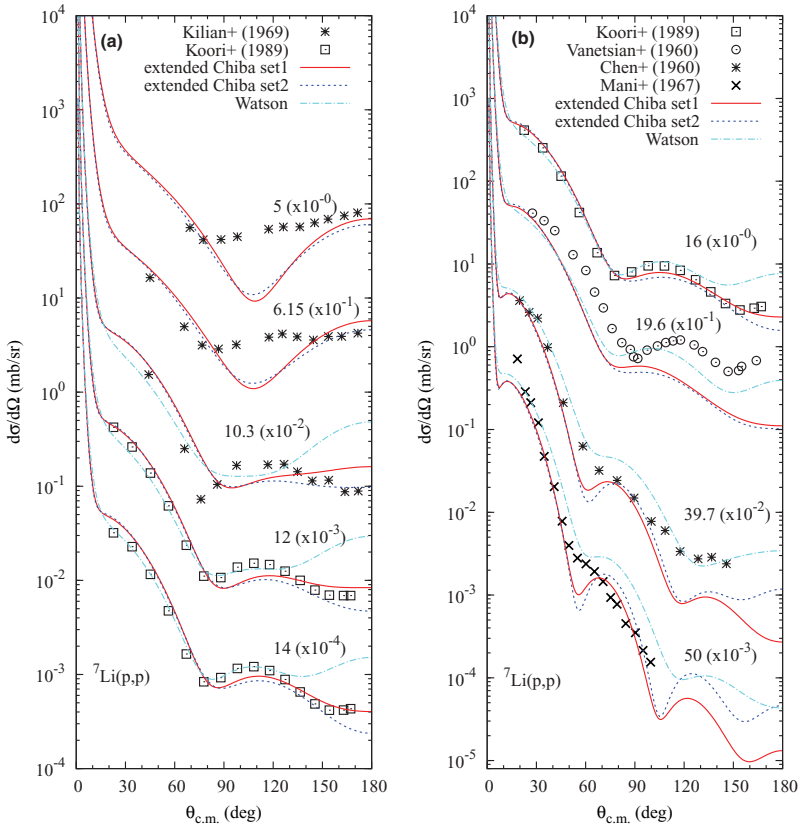

FIG. 4. (Color online) The same as in Fig. 2 but for the target nucleus ^{7}Li.

necessarily yield satisfactory agreement with experimental data of both nucleon and deuteron elastic scattering from ^{6,7}Li for energies up to 50 MeV. Thus, the present work is devoted to finding the most appropriate nucleon OMP for ^{6,7}Li from optical model analysis of differential cross sections of nucleon elastic scattering, neutron total cross sections, and reaction cross sections of ^{6,7}Li. The obtained nucleon OMP is finally validated by the CDCC analysis of deuteron elastic scattering and reaction cross sections.

Section II describes the methodology of extracting the nucleon OMP of ^{6,7}Li. Section III presents our results and discussion: The optical model calculations of nucleon elastic scattering, neutron total cross sections, and reaction cross sections for ^{6,7}Li are compared with experimental data. Comparisons between experimental data and CDCC calculations for deuteron elastic scattering from ^{6,7}Li are presented together with the optical model calculation using a phenomenological deuteron OMP of Avrigeanu *et al.* [16]. The effects of the deuteron spin and breakup states on CDCC calculations are also discussed. Finally, conclusions are given in Sec. IV.

II. NUCLEON OPTICAL POTENTIAL OF LITHIUM

There are few currently available OMPs for both neutrons and protons for ^{6,7}Li that cover the whole energy range of 5 to 25 MeV of interest. A neutron optical potential for $1p$ shell nuclei derived by Dave and Gould [14] is one of the candidates for energies below 15 MeV. However, it significantly overestimates neutron total cross sections for energies above 15 MeV. Therefore, we cannot apply the Dave-Gould OMP to our CDCC analysis up to 50 MeV because the nucleon OMP is required for energies up to 25 MeV in the CDCC calculations. The global nucleon OMP of Watson *et al.* [15] for $1p$ shell nuclei is also available at energies between 10 and 50 MeV, although the agreement with experimental (p, p) scattering is not necessarily satisfactory, as shown in Fig. 8 of Ref. [15]. The neutron OMP of ^{6}Li proposed by Chiba *et al.* [17] is the latest one that is applicable to the energy range from 5 to several tens of MeV. The optical model calculation with the potential can reproduce fairly well experimental data of both neutron total cross sections and differential cross sections of neutron elastic scattering from ^{6}Li.

For the measurements, there are many experimental data of neutron total cross sections and differential cross sections of neutron elastic scattering from ^{6,7}Li in the energy range of our interest, but only a few reaction cross section data with rather large uncertainties exist. However, it should be noted that all neutron elastic scattering data of ^{7}Li include the inelastic scattering contribution from the first excited state ($E_{\rm ex} =$ 0.478 MeV), because experimental energy resolution is not good enough to separate the levels. This indicates that it may be difficult to find a reliable neutron OMP for ^{7}Li from the elastic scattering data by a conventional method of searching OMP parameters.

Given the situation for the nucleon OMPs of ^{6,7}Li, we propose a method to determine both the neutron and proton OMPs of ^{6,7}Li in a consistent way using the Chiba OMP [17].

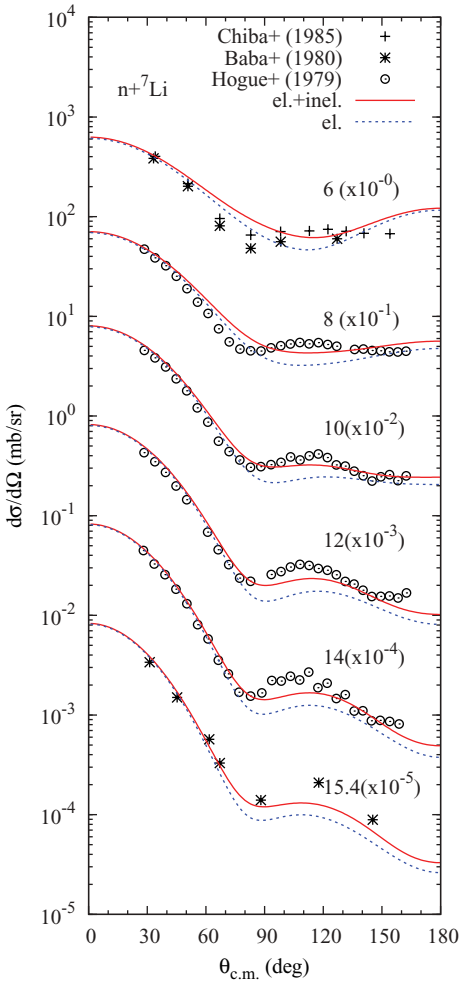

FIG. 5. (Color online) Contribution of neutron inelastic scattering to the excited state ($E_{\rm ex} = 0.478$ MeV) for ^{7}Li. The inelastic cross sections are taken from the JENDL-3.3 nuclear data library [22]. The solid curves present the sum of the inelastic scattering cross sections and the elastic scattering cross sections calculated by using the extended Chiba OMP with the Set 1 parameter shown by short-dashed curves.

We choose the same spherical optical potential as used in the Chiba OMP, namely,

$$U = -(V_r + iW_v) f(r, r_v, a_v) + 4ia_d W_d \frac{d}{dr} f(r, r_d, a_d) + \left(\frac{\hbar}{m_\pi c}\right)^2 (\boldsymbol{l}\cdot\boldsymbol{s}) V_{\rm so} \frac{1}{r}\frac{d}{dr} f(r, r_{\rm so}, a_{\rm so}). \quad (1)$$

In this equation, f is the Woods-Saxon form factor given by

$$f(r, r_x, a_x) = \frac{1}{1 + \exp\left(\frac{r - r_x A^{1/3}}{a_x}\right)}, \quad (2)$$

where r_x and a_x ($x = v, d$, so) are the radius and diffuseness parameters, respectively, and A is the target mass number.

Since both neutron and proton OMPs of ^{6,7}Li are necessary in the CDCC analysis of deuteron elastic scattering, we extend the neutron OMP to the proton OMP by including the Lane potential [18], and we further extend them to include the ^{7}Li

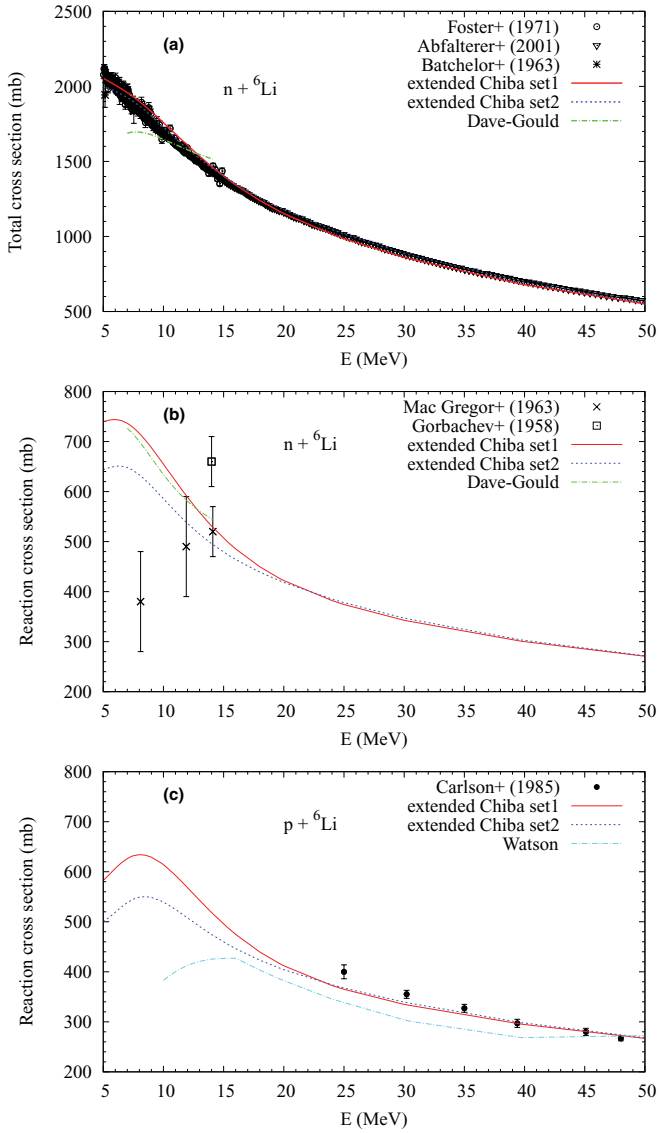

FIG. 6. (Color online) Comparison of the experimental data and optical model calculations for (a) neutron total cross sections, (b) neutron reaction cross sections, and (c) proton reaction cross sections for ^{6}Li. The solid and short-dashed curves represent the calculations using the extended Chiba OMP with the Set 1 and Set 2 parameters, respectively. The dash-dotted curves are the results of the Dave-Gould OMP (neutron) and the Watson OMP (proton).

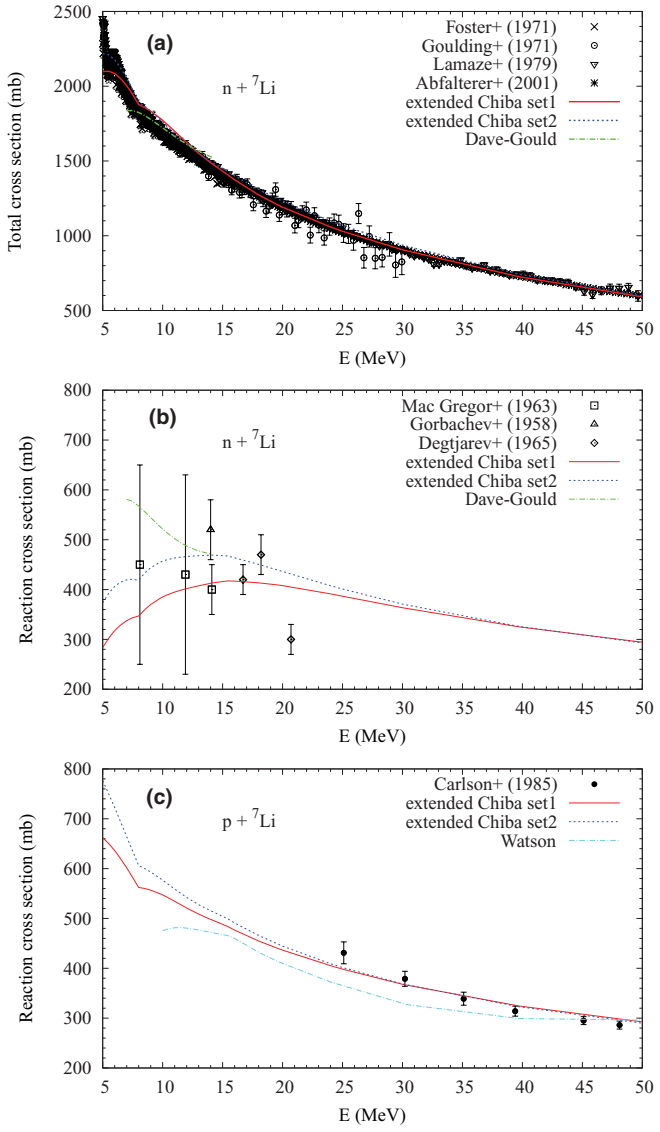

FIG. 7. (Color online) The same as in Fig. 6 but for the target nucleus ^{7}Li.

target by changing the Fermi energies. Hereafter this extended version will be referred to as the extended Chiba OMP. The depth parameters of the OMP are given as a function of the incident nucleon energy E_N:

$$V_r = \left(V_0 + V_1 \pm 21\frac{N-Z}{A}\right)\left[1 - \frac{V_0(1 - e^{-\lambda_v(E_N - E_f)})}{V_0 + V_1}\right] + [\Delta V_C(E_N)]_{\text{for protons}}, \tag{3}$$

$$W_d = \left(W_{d_0} \pm 16\frac{N-Z}{A}\right) e^{-\lambda_{W_d}(E_N - E_f)} \frac{(E_N - E_f)^4}{(E_N - E_f)^4 + W_{d_1}^4}, \tag{4}$$

$$W_v = W_{v_0}\frac{(E_N - E_f)^4}{(E_N - E_f)^4 + W_{v_1}^4}, \tag{5}$$

$$V_{\text{so}} = V_{\text{so}_0} e^{-\lambda_{\text{so}}(E_N - E_f)}, \tag{6}$$

where the $(N-Z)/A$ term is the isospin dependence term, $\Delta V_C(E_N)$ is the Coulomb correction term for the proton OMP, which is given by Eq. (23) of Ref. [13], and E_F is the Fermi energy. In the $(N-Z)/A$ term, the plus and minus signs indicate proton and neutron OMPs, respectively, and the coefficients come from the Koning-Delarosche OMP [13].

The Fermi energy is calculated by using the following expressions:

$$E_{f_n} = -\tfrac{1}{2}[S_n(A) + S_n(A+n)] \quad \text{for neutrons}, \tag{7}$$

$$E_{f_p} = -\tfrac{1}{2}[S_p(A) + S_p(A+p)] \quad \text{for protons}, \tag{8}$$

TABLE I. Nucleon optical model potential parameters of ^{6,7}Li. V_x, W_x, and E_N are given in MeV, λ_x in MeV^{-1}, and r_x and a_x in femtometers.

Parameter	Set 1	Set 2
V_0	65.64	71.68
V_1	−26.71	−29.69
λ_v	0.00486	0.00495
r_v	^{7}Li: $\begin{cases} 1.55 - 0.035E_N, & E_N \in [5, 8) \\ 1.19 + 0.01E_N, & E_N \in [8, 15) \\ 1.34, & E_N \in [15, 50] \end{cases}$ ^{6}Li: 1.34	^{7}Li: $\begin{cases} 1.46 - 0.04E_N, & E_N \in [5, 8) \\ 1.04855 + 0.01143E_N, & E_N \in [8, 15) \\ 1.22, & E_N \in [15, 50] \end{cases}$ ^{6}Li: 1.22
a_v	0.707	0.822
W_{v_0}	10.19	10.06
W_{v_1}	18.42	14.03
W_{d_0}	$\begin{cases} 74.69 & (^6\text{Li}) \\ 16.0 & (^7\text{Li}) \end{cases}$	$\begin{cases} 321.4 & (^6\text{Li}) \\ 16.0 & (^7\text{Li}) \end{cases}$
W_{d_1}	15.69	18.76
λ_{W_d}	0.207	0.315
r_d	1.59	1.37
a_d	0.899	0.699
V_{so_0}	8.374	8.702
λ_{so}	0.01407	0.01407
r_{so}	1.58	1.64
a_{so}	0.427	0.311

where $S_y(X)$ is the separation energy of y (= neutron or proton) from the target X. Finally, the Fermi energies of protons and neutrons for ^{6,7}Li are given as

$$\begin{aligned} E_{f_n}(^6\text{Li}) &= -6.457 \text{ MeV}, \\ E_{f_n}(^7\text{Li}) &= -4.641 \text{ MeV}, \\ E_{f_p}(^6\text{Li}) &= -5.099 \text{ MeV}, \\ E_{f_p}(^7\text{Li}) &= -13.62 \text{ MeV}. \end{aligned} \tag{9}$$

III. RESULTS AND DISCUSSION

A. Nucleon elastic scattering from ^{6,7}Li

The extended Chiba OMP is applied to calculate cross sections of nucleon elastic scattering from ^{6,7}Li. The ECIS code [19] is employed in the calculations. Two parameter sets of the Chiba OMP (called Set 1 and Set 2) are used, because they make a little difference in agreement with experimental ^{6}Li(n, n) data, as shown in Ref. [17]. All the adopted parameter values are the same as those of Ref. [17] except for two, r_v and W_{d_0}, which are adjusted to obtain better agreement with experimental data. According to Delaroche *et al.* [20], the radius parameter of the real volume term, r_v, is assumed to have a weak energy dependence. Hence, r_v is slightly adjusted so that experimental data of neutron total and reaction cross sections and elastic scattering angular distributions can be reproduced reasonably well. The imaginary surface depth, W_{d_0}, is also adjusted for ^{7}Li to reproduce the experimental proton elastic scattering angular distributions. All the parameters determined in the present work are listed in Table I.

In Figs. 1 to 7, optical model calculations with the extended Chiba OMP are compared with experimental data and those with other global OMPs, that is, the Dave-Gould OMP [14] for neutrons and the Watson OMP [15] for protons. In the calculations with the Dave-Gould OMP, the individual parameter sets (Table II in Ref. [14]) are applied to ^{6}Li and ^{7}Li, because they reproduce the experimental data better than the global parameter set. The experimental data are taken from the EXFOR data base [21] and other references (which are listed in Table II). As mentioned in Sec. III, the neutron elastic scattering data of ^{7}Li contain the contribution from inelastic scattering to the first excited state ($E_{ex} = 0.478$ MeV). Therefore, it is necessary to estimate the inelastic scattering component to compare our calculations with the measurements. In the present work, the inelastic differential cross sections stored in the JENDL-3.3 nuclear data library [22] for energies up to 20 MeV are added to the calculated elastic ones. In JENDL-3.3, the inelastic cross sections were evaluated on the basis of the $(n, n'\gamma)$ data of Morgan [23] and the angular distributions were given by using a coupled-channels calculation, in which the symmetric rotational model was assumed and the coupling scheme was taken as 3/2(g.s.)-1/2(0.478)-7/2(4.63)-5/2(6.68) in the $K = 1/2$ band [24]. The sum of the elastic and inelastic differential cross sections are plotted in Fig. 3. Only the elastic scattering component is presented by the short-dashed curve in Fig. 5 to show the contribution from the inelastic scattering in the calculation result given by the solid curve in Fig. 3.

For nucleon elastic scattering, the calculation with the extended Chiba OMP is in overall good agreement with the

TABLE II. Experimental data of nucleon elastic scattering angular distributions, total cross sections ("tot"), and reaction cross sections ("non").

Reactions	Ref.	Energy (MeV)
^{6}Li(n, n)	[28]	5, 6, 7, 7.5
	[29]	7.5, 9, 10, 11, 12, 12.9, 13.9
	[17]	11.5, 14.1, 18
	[30]	14.1
	[31]	24
^{6}Li(p, p)	[32]	5, 6, 7, 8
	[33]	5, 6, 7, 8, 11, 12
	[34]	14
	[35]	19.6
	[36]	39.7
	[37]	50
^{6}Li(n,tot)	[38–40]	5–50
^{6}Li(n,non)	[41,42]	8.1, 11.9, 14, 14.1
^{6}Li(p,non)	[43]	25, 30.2, 35, 39.4, 45.1, 48
^{7}Li(n, n)	[44]	5, 6, 15.4
	[45]	6, 14
	[46]	11
	[29]	7, 8, 9, 10, 11, 12, 13, 14
	[31]	24
^{7}Li(p, p)	[47]	5, 6.15, 10.3
	[34]	12, 14, 16
	[35]	19.6
	[36]	39.7
	[37]	50
^{7}Li(n,tot)	[38,39,48,49]	5–50
^{7}Li(n,non)	[41,42,50]	8.1, 11.9, 14, 14.1, 16.7, 18.2, 20.7
^{7}Li(p,non)	[43]	25.1, 30.2, 35.1, 39.4, 45.1, 48.1

experimental data for energies up to 50 MeV as shown in Figs. 1 to 4. The result with the Set 2 parameter looks slightly better than that with the Set 1 parameter for ^{6}Li, particularly at low energies in Fig. 1, whereas the calculation with the Set 1 parameter shows better agreement with the measurement than that with the Set 2 parameter at large angles for ^{7}Li in Fig. 3. Use of the Dave-Gould OMP leads to better agreement with the experimental data around intermediate angles in the applicable energy range of 7 to 15 MeV than that of the extended Chiba OMP in Figs. 1 and 3. The calculation with the Watson OMP deviates considerably form the experimental (p, p) data for both ^{6}Li and ^{7}Li (Figs. 2 and 4). A large discrepancy between the calculation and the measurement is found in ^{6,7}Li(p, p) scattering at 19.6 MeV. The reason is not clear at present. Also, the calculation reproduces the measurement poorly in the middle angular range in ^{7}Li(p, p) scattering at 5 and 6.15 MeV, which might be improved by taking into account compound elastic scattering.

As shown in Figs. 6 and 7, the calculation with the extended Chiba OMP shows excellent agreement with measured neutron total cross sections over the whole energy range. A difference is seen between the reaction cross sections calculated with the Set 1 and Set 2 parameters at energies below 20 MeV, which is due mainly to the difference in the imaginary part. Although there are some experimental data of neutron reaction cross sections, we cannot discuss the relative merits, because they have large errors. Both the proton reaction cross sections calculated with the Set 1 and Set 2 parameters converge at energies above 25 MeV, reproducing the experimental data better than those with the Watson OMP.

By considering these comparisons comprehensively, we conclude that the extended Chiba OMP is the most appropriate OMP between the nucleon and ^{6,7}Li over the wide energy range from 5 to 50 MeV. In the next section, the extended Chiba OMP will be applied to CDCC calculations of deuteron elastic scattering and reaction cross sections for ^{6,7}Li.

B. Deuteron elastic scattering from ^{6,7}Li

Differential cross sections of deuteron elastic scattering from ^{6,7}Li and total reaction cross sections for incident energies between 9 and 50 MeV are calculated by using the set of CDCC codes consisting of CDCDEU, HICADEU, and XPOLADEU [25], which have been developed on the basis of the CDCC method [6,7].

1. Input of CDCC calculation

The extended Chiba OMP is chosen as the nucleon OMP at half the incident deuteron energy in CDCC calculations. The spin of the deuteron, $I = 1$, is considered explicitly and both the central and spin-orbit terms of the nucleon optical potentials are included. The deuteron ground-state wave function is composed of the $^3S_1$ state alone, and the mixture of D states is neglected. The breakup state wave functions contain the relative angular momentum of the p-n subsystem, $\ell = 0$ and 2 (i.e., $^3S_1$, $^3D_1$, $^3D_2$, and $^3D_3$). The wave functions of the ground state and breakup states are constructed by using a Gaussian potential [26]. The calculated root mean square of the radius of the deuteron ($\langle r \rangle_d^{1/2}$) is 1.926 fm, whereas the experimental data give a value of 1.9635 fm [27]. The contribution from closed channels is neglected, which means that the maximum linear momentum for each incident energy is given by

$$k_{\max} = \frac{\sqrt{2\mu_\rho \left(E_d^{(\mathrm{cm})} - |\varepsilon_0|\right)}}{\hbar}, \tag{10}$$

where μ_ρ is the reduced mass of the p-n subsystem, ε_0 is the deuteron binding energy, and $E_d^{(\mathrm{cm})}$ is the deuteron incident energy in the center-of-mass frame of the deuteron-target system. The maximum total angular momentum $J_{\max}$ is set to 20, and the total number of the discretized continuum bins, $N_{\max}$, is set to 12. It was confirmed that the adopted values of $J_{\max}$ and $N_{\max}$ are enough to obtain the convergence of CDCC calculations.

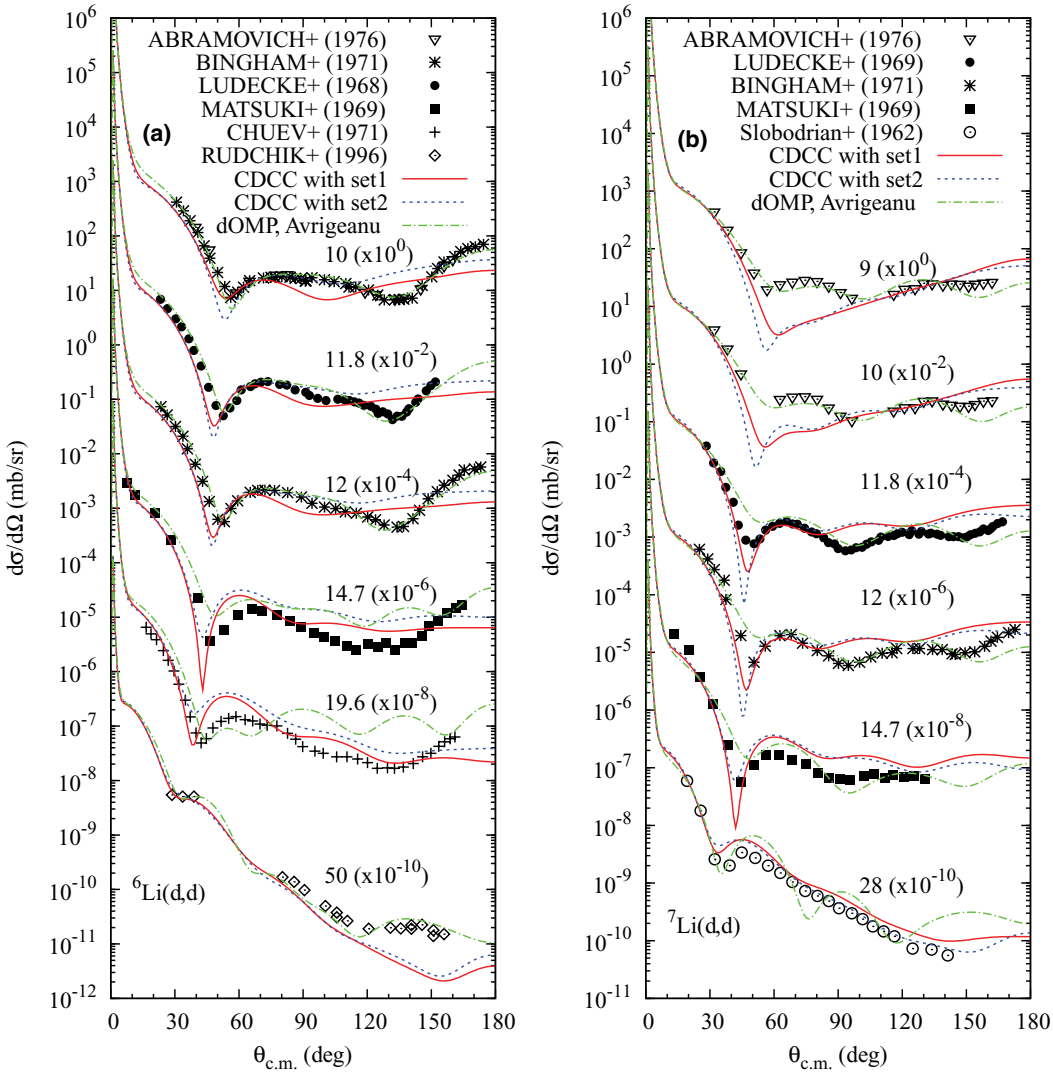

FIG. 8. (Color online) Comparison of the experimental and calculated differential cross sections of deuteron elastic scattering from (a) ^{6}Li and (b) ^{7}Li. The solid and short-dashed curves are the CDCC results using the extended Chiba OMP with the Set 1 and Set 2 parameters, respectively. The dash-dotted curves are the optical model calculation with the Avrigeanu OMP. The number at the top of each plot denotes incident energy in MeV.

2. *Result of CDCC analysis*

Figure 8 shows the CDCC calculation for deuteron elastic scattering from ^{6,7}Li along with experimental data and optical model calculation using the deuteron OMP [16]. References of the experimental data are listed in Table III. The CDCC calculation reproduces the measurements well to the same extent as the optical model calculation does, although a large discrepancy is seen in the middle angular range at incident energies of 9 and 10 MeV for ^{7}Li. Both the CDCC calculations with different parameter sets, Set 1 and Set 2, are almost same over the whole angular range except in the vicinity of the first minimum seen in the angular distributions.

CDCC total reaction cross sections of ^{6,7}Li are shown in Fig. 9 along with the optical model calculation using the Avrigeanu OMP [16]. Since there is no available measurement of ^{6,7}Li, the calculations are compared with experimental data of ^{9}Be multiplied by the scaling factors that are obtained under

TABLE III. Experimental data of deuteron elastic scattering.

Target	Ref.	Energy (MeV)
^{6,7}Li	[51]	11.8
	[52]	12
	[53]	14.7
^{6}Li	[51]	10
	[54]	19.6
	[55]	50
^{7}Li	[56]	9, 10
	[57]	28

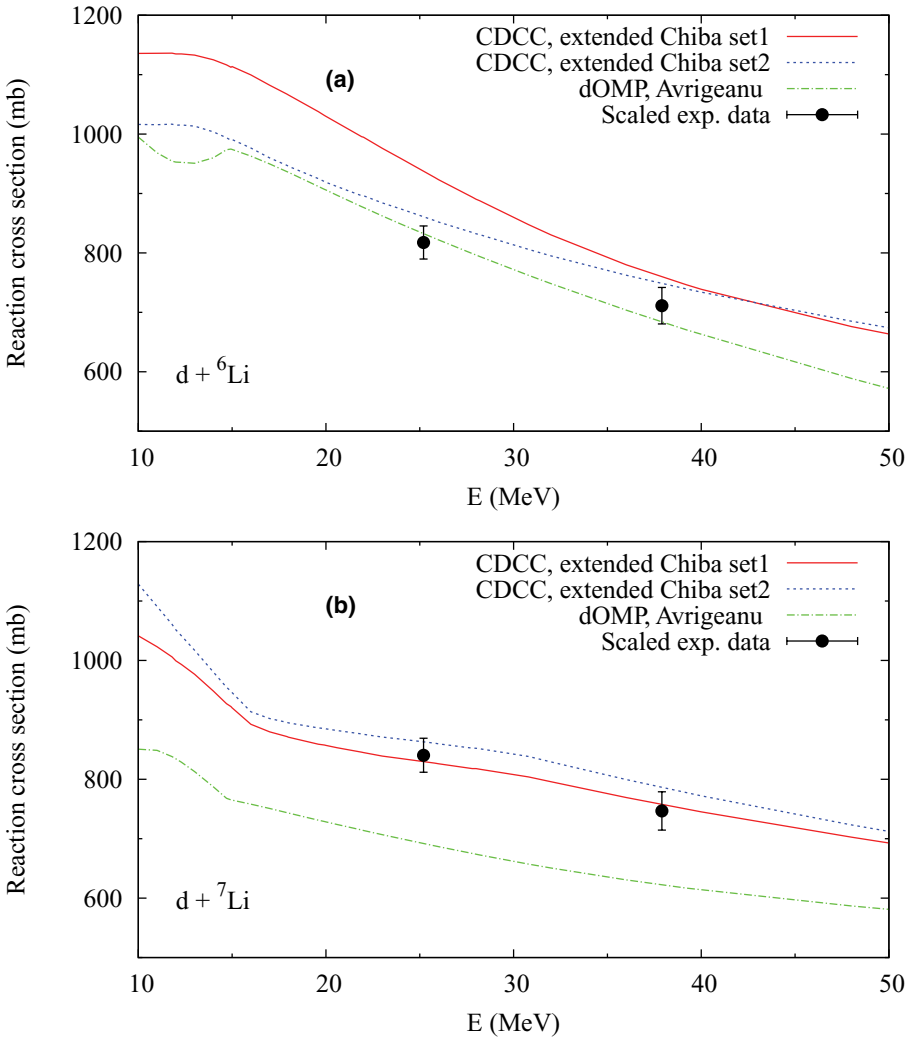

FIG. 9. (Color online) Reaction cross sections for deuteron incident on (a) ^{6}Li and (b) ^{7}Li as a function of incident energy. The solid and short-dashed curves are the CDCC results using the extended Chiba OMP with the Set 1 and Set 2 parameters, respectively. The dash-dotted curves are the optical model calculations using the Avrigeanu deuteron OMP. The closed circles are the "scaled" experimental data of ^{9}Be explained in the text.

an assumption that the reaction cross section is described approximately by Eq. (4) of Ref. [58]. Namely, the "scaled" experimental reaction cross section is given by

$$\sigma_R^{\text{scaled}}(^{6,7}\text{Li}) = \frac{\sigma_R^{\text{emp}}(^{6,7}\text{Li})}{\sigma_R^{\text{emp}}(^{9}\text{Be})}\sigma_R^{\text{exp}}(^{9}\text{Be}), \tag{11}$$

where σ_R^{emp} is the empirical reaction cross section expressed as a function of the target mass number with incident-energy-dependent parameters [58] and σ_R^{exp} is the experimental data of ^{9}Be [58,59]. In the case of ^{6}Li, the CDCC cross sections calculated with the Set 1 parameter are larger than those with the Set 2 parameter at energies below 40 MeV, which is due mainly to the difference in the imaginary part of the extended Chiba OMP. The "scaled" experimental data are close to the CDCC calculation with the Set 2 parameter and the optical model calculation. Meanwhile, both the CDCC cross sections calculated with the Set 1 and Set 2 parameters are similar for ^{7}Li and are obviously larger than the optical model calculation with the Avrigeanu OMP over the whole energy range, showing better agreement with the "scaled" experimental data. Thus, it is found that the CDCC calculation with the extended Chiba OMP reproduces the "scaled" experimental data successfully for both ^{6}Li and ^{7}Li. However, direct measurements of reaction cross sections for ^{6,7}Li will be desirable for further validation.

In the present CDCC calculation, the deuteron spin $I = 1$ is taken into account, but the spin was assumed to be zero in the previous CDCC analysis of (d, d) scattering from medium-heavy nuclei [12]. It is interesting to see the effect of the deuteron spin on CDCC calculations. A comparison between the results with $I = 1$ and $I = 0$ is shown for ^{6}Li(d, d) scattering in Fig. 10. The extended Chiba OMP with the Set 2 parameter is used. Some differences appear at middle and backward angles, although there is no appreciable difference at forward angles smaller than the first minimum. The calculated angular distributions with $I = 0$ show a more oscillated shape at middle and backward angles with decreasing incident energy than those with $I = 1$, and better agreement with the measurement is seen at angles larger than 150 degrees. For the highest incident energy of 50 MeV, the calculation with $I = 1$ leads to a significant increase in the cross section at backward

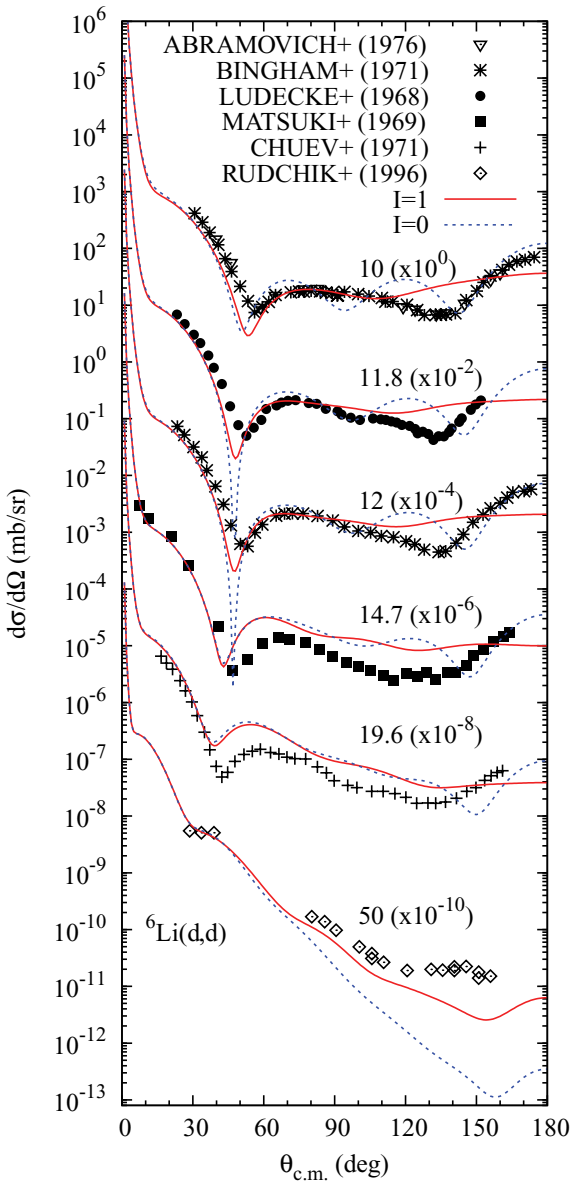

FIG. 10. (Color online) Comparison of the CDCC calculations with deuteron spin $I = 1$ (solid curves) to that with $I = 0$ (short-dashed curves) for deuteron elastic scattering from ^{6}Li. The extended Chiba OMP with the Set 2 parameter is used in both calculations. The number at the top of each plot denotes incident energy in MeV.

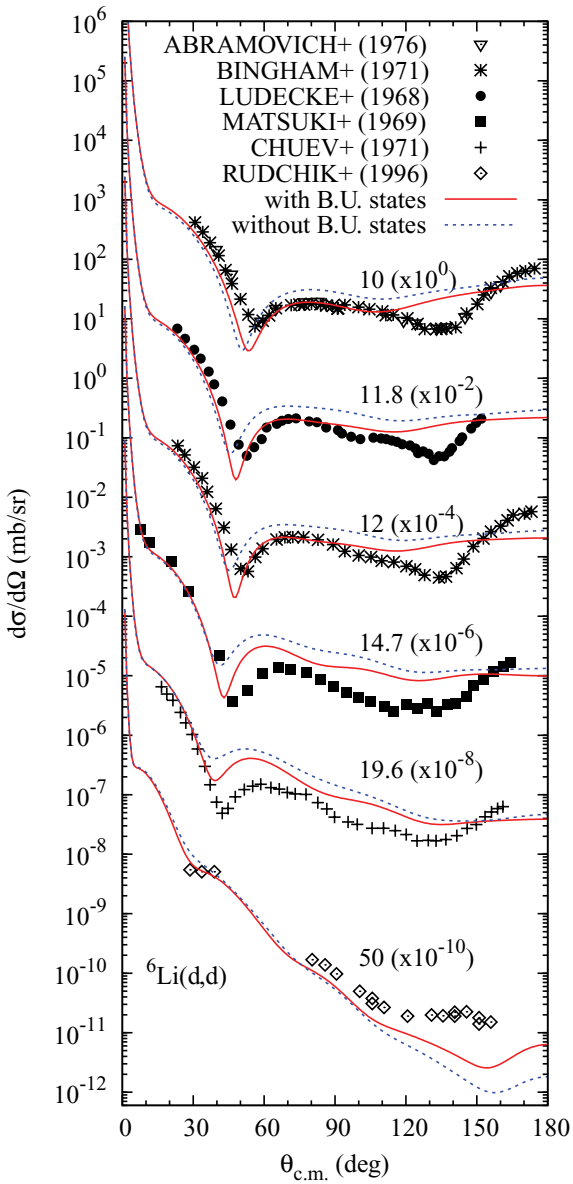

FIG. 11. (Color online) Comparison of the CDCC calculations including deuteron breakup states (solid curves) and that including only the ground state (short-dashed curves) for deuteron elastic scattering from ^{6}Li. The extended Chiba OMP with the Set 2 parameter is used in both calculations. The number at the top of each plot denotes incident energy in MeV.

angles and agreement with the experimental data is improved. It should be noted that the tendency seen for ^{6}Li is true of ^{7}Li.

Finally, the effect of deuteron breakup on elastic scattering is examined. The result is shown for ^{6}Li(d, d) at energies from 10 to 50 MeV in Fig. 11, where the extended Chiba OMP with the Set 2 parameter is used. The solid curves are the same as in Fig. 8. The dotted curve presents the calculation that takes account of the deuteron ground state alone. The comparison shows that inclusion of the continuum states of the deuteron leads to a reduction of the differential cross sections at large angles, and better agreement with the measurement is obtained. This suggests the importance of the deuteron breakup effect in deuteron elastic scattering.

IV. SUMMARY AND CONCLUSIONS

The phenomenological nucleon optical model potential of ^{6,7}Li was determined for energies from 5 to 50 MeV by extending the neutron OMP of ^{6}Li given by Chiba *et al.* [17] in a consistent way based on the Lane model. It was confirmed that the optical model calculation with the extended Chiba OMP can describe well the nucleon angular distributions and neutron total cross sections of ^{6,7}Li.

The extended Chiba OMP was applied to the CDCC analysis of deuteron elastic scattering up to 50 MeV. The calculation shows reasonable overall agreement with the experimental angular distributions. Particularly good agreement is obtained at forward angles to the same extent as the optical model calculation with the phenomenological deuteron OMP [16]. In addition, the calculated reaction cross sections for both ^{6}Li and ^{7}Li reproduce fairly well the "scaled" experimental data, which are estimated by using the empirical formula of the reaction cross section and the experimental data of ^{9}Be, compared to the optical model prediction. Therefore, it is expected that the CDCC calculation of deuteron elastic scattering and reaction cross sections will be helpful to validate the nucleon OMPs and to impose additional constraints on them.

The importance of projectile breakup effects in deuteron elastic scattering from ^{6,7}Li was also confirmed in the present CDCC analysis. The successful application of the CDCC method to deuteron elastic scattering encourages us to employ it to predict neutrons produced by deuteron breakup processes. The prescription for the (d, pn) reaction has already been established by Iseri *et al*. [7] and the code is now available [25]. As a next step, we plan to clarify the importance of deuteron breakup processes in inclusive Li(d, xn) reactions up to 50 MeV quantitatively by a CDCC calculation with the extended Chiba OMP.

ACKNOWLEDGMENTS

We would like to thank M. Kawai, M. Yahiro, M. Kamimura, and Y. Iseri for helpful discussions and comments on our CDCC analyses. This work was supported by a Grant-in-Aid for Scientific Research of the Japan Society for the Promotion of Science (No. 19560844).

[1] H. Matsui, in *Proceedings of the 23rd Symposium on Fusion Technology*, Venice, Italy, 20–24 September 2004.
[2] M. Hagiwara, T. Itoga, N. Kawata, N. Hirabayashi, T. Oishi, T. Yamauchi, M. Baba, M. Sugimoto, and T. Muroga, Fusion Sci. Technol. **48**, 1320 (2005).
[3] A. Yu. Konobeyev, Yu. A. Korovin, P. E. Pereslavtsev, U. Fischer, and U. von Möllendorff, Nucl. Sci. Eng. **139**, 1 (2001).
[4] U. Fischer, M. Avrigeanu, P. Pereslavtsev, S. P. Simakov, and I. Schmuck, J. Nucl. Mat. **367**, 1531 (2007).
[5] R. Serber, Phys. Rev. **72**, 1008 (1947).
[6] M. Yahiro, Y. Iseri, H. Kameyama, M. Kamimura, and M. Kawai, Prog. Theor. Phys. Suppl. **89**, 32 (1986).
[7] Y. Iseri, M. Yahiro, and M. Kamimura, Prog. Theor. Phys. Suppl. **89**, 84 (1986).
[8] K. Ogata, M. Yahiro, Y. Iseri, and M. Kamimura, Phys. Rev. C **67**, 011602(R) (2003).
[9] K. Ogata, M. Yahiro, Y. Iseri, T. Matsumoto, and M. Kamimura, Phys. Rev. C **68**, 064609 (2003).
[10] J. A. Tostevin, F. M. Nunes, and I. J. Thompson, Phys. Rev. C **63**, 024617 (2001).
[11] K. Ogata, S. Hashimoto, Y. Iseri, M. Kamimura, and M. Yahiro, Phys. Rev. C **73**, 024605 (2006).
[12] P. Chau Huu-Tai, Nucl. Phys. **A773**, 56 (2006).
[13] A. J. Koning and J. P. Delaroche, Nucl. Phys. **A713**, 231 (2003).
[14] J. H. Dave and C. R. Gould, Phys. Rev. C **28**, 2212 (1983).
[15] B. A. Watson, P. P. Singh, and R. E. Segel, Phys. Rev. **182**, 977 (1969).
[16] M. Avrigeanu, W. von Oertzen, U. Fischer, and V. Avrigeanua, Nucl. Phys. **A759**, 327 (2005).
[17] S. Chiba, K. Togasaki, M. Ibaraki, M. Baba, S. Matsuyama, N. Hirakawa, K. Shibata, O. Iwamoto, A. J. Koning, G. M. Hale, and M. B. Chadwick, Phys. Rev. C **58**, 2205 (1998).
[18] A. M. Lane, Nucl. Phys. **35**, 676 (1962).
[19] J. Raynal, in *Proceedings of the Specialists' Meeting on the Nucleon Nucleus Optical Model up to 200 MeV*, Bruyres-le-Chatel, France, 13–15 November 1996.
[20] J. P. Delaroche, Y. Wang, and J. Rapaport, Phys. Rev. C **39**, 391 (1989).
[21] http://www-nds.iaea.or.at/exfor/exfor00.htm.
[22] K. Shibata, T. Kawano, T. Nakagawa, O. Iwamoto, J. Katakura, T. Fukahori, S. Chiba, A. Hasegawa, T. Murata, H. Matsunobu, T. Ohsawa, Y. Nakajima, T. Yoshida, A. Zuckeran, M. Kawai, M. Baba, M. Ishikawa, T. Asami, T. Watanabe, Y. Watanabe, M. Igashira, N. Yamamuro, H. Kitazawa, N. Yamano, and H. Takano, J. Nucl. Sci. Technol. **39**, 1125 (2002); http://wwwndc.jaea.go.jp/jendl/j33/j33.html.
[23] G. L. Morgan, ORNL/TM-6247, Oak Ridge National Laboratory, 1978; EXFOR-10788 data file entry.
[24] S. Chiba and K. Shibata, JAERI-M 88-164, 1988.
[25] Y. Iseri, M. Kamimura, M. Yahiro, Y. Sakuargi, and K. Ogata, Bull. Res. Comput. Syst. Comput. Commun. Cent. Kyushu Univ. **5**(3), 117 (2006) (CDCDEU); **1**(1), 16 (2007) (HICADEU); **1**(3), 88 (2008) (XPOLADEU).
[26] R. V. Reid Jr., Ann. Phys. (NY) **50**, 411 (1968).
[27] O. Dumbrajs, R. Koch, H. Pilkuhn, G. C. Oades, H. Behrens, J. J. de Swart, and P. Kroll, Nucl. Phys. **B216**, 277 (1983).
[28] H. D. Knox, R. M. White, and R. O. Lane, Nucl. Sci. Eng. **69**, 223 (1979); EXFOR-10710 data file entry.
[29] H. H. Hogue, P. L. von Behren, D. W. Glasgow, S. G. Glendinning, P. W. Lisowski, C. E. Nelson, F. O. Purser, W. Tornow, C. R. Gould, and L. W. Seagondollar, Nucl. Sci. Eng. **69**, 22 (1979); EXFOR-10707 data file entry.
[30] M. Hyakutake, M. Sonoda, A. Katase, Y. Wakuta, M. Matoba, H. Tawara, and I. Fujita, J. Nucl. Sci. Technol. **11**, 407 (1974); EXFOR-20268 data file entry.
[31] L. F. Hansen, J. Rapaport, X. Wang, F. A. Barrios, F. Petrovich, A. W. Carpenter, and M. J. Threapleton, Phys. Rev. C **38**, 525 (1988); EXFOR-13161 data file entry.
[32] M. Haller, W. Kretschmer, A. Rauscher, R. Schmitt, and W. Schuster, Nucl. Phys. **A496**, 189 (1989); EXFOR-F0063 data file entry.
[33] W. D. Harrison and A. B. Whirehead, Phys. Rev. **132**, 2607 (1963); EXFOR-C1003 data file entry.
[34] N. Koori, I. Kumabe, M. Hyakutake, K. Orito, K. Akagi, A. Iida, Y. Watanabe, K. Sagara, H. Nakamura, K. Maeda, T. Nakashima, M. Kamimura, and Y. Sakuragi, JEARI-M 89-167, 1989.
[35] R. A. Vanetsian, A. P. Klyucharev, and E. D. Fedchenko, Sov. At. Energ. **6**, 490 (1960).

[36] S. Chen and N. M. Hintz, in *International Conference on Nuclear Forces and the Few Nucleon Problem*, edited by T. C. Griffith and E. A. Power (Pergamon Press, New York, 1960), p. 683.
[37] G. S. Mani, A. D. B. Dix, D. T. Jones, and M. Richardson, Rutherford Laboratory Report No. RHEL/R-136, 1967 (unpublished), p. 49.
[38] D. G. Foster Jr. and D. W. Glasgow, Phys. Rev. C **3**, 576 (1971); EXFOR-10047 data file entry.
[39] W. P. Abfalterer, F. B. Bateman, F. S. Dietrich, R. W. Finlay, R. C. Haight, and G. L. Morgan, Phys. Rev. C **63**, 044608 (2001); EXFOR-13753 data file entry.
[40] R. Batchelor and J. H. Towle, Nucl. Phys. **47**, 385 (1963); EXFOR-21147 data file entry.
[41] M. H. Mac Gregor, R. Booth, and W. P. Ball, Phys. Rev. **130**, 1471 (1963); EXFOR-11120 data file entry.
[42] V. M. Gorbachev and L. B. Poretskii, Sov. At. Energ. **4**, 259 (1958); EXFOR-40391 data file entry.
[43] R. F. Carlson, A. J. Cox, T. N. Nasr, M. S. De Jong, D. L. Ginther, D. K. Hasell, A. M. Sourkes, W. T. H. van Oers, and D. J. Margaziotis, Nucl. Phys. **A445**, 57 (1985); EXFOR-C0215 data file entry.
[44] M. Baba, N. Hayashi, T. Sakase, T. Iwasaki, S. Kamata, and T. Momota, Bull. Am. Phys. Soc. **24**, 862 (1979); EXFOR-21630 data file entry.
[45] S. Chiba, M. Baba, H. Nakashima, M. Ono, N. Yabuta, S. Yukinori, and N. Hirakawa, J. Nucl. Sci. Technol. **22**, 771 (1985); EXFOR-21986 data file entry.
[46] S. Chiba, Y. Yamanouti, M. Mizumoto, M. Hyakutake, and S. Iwasaki, J. Nucl. Sci. Technol. **25**, 210 (1988); EXFOR-22082 data file entry.
[47] K. Kilian, G. Clausnitzer, W. Dürr, D. Fick, R. Fleischmann, and H. M. Hofmann, Nucl. Phys. **A126**, 529 (1969); EXFOR-A1443 data file entry.
[48] C. A. Goulding, P. Stoler, and J. M. Clement, EXFOR-10251 data file entry.
[49] G. P. Lamaze, J. D. Kellie, and R. B. Schwartz, in *Proceedings of the International Conference on Nuclear Cross Sections for Technology*, edited by J. L. Fowler, C. H. Johnson, and C. D. Bowman (University of Tennessee, Knoxville, 1979), p. 48; EXFOR-10888 data file entry.
[50] Ju. G. Degtjarev, Sov. At. Energ. **19**, 1426 (1965); EXFOR-40694 data file entry.
[51] H. Ludecke, T. Wan-Tjin, H. Werner, and J. Zimmerer, Nucl. Phys. **A109**, 676 (1968); EXFOR-F0002 data file entry.
[52] H. G. Bingham, A. R. Zander, K. W. Kemper, and N. R. Fletcher, Nucl. Phys. **A173**, 265 (1971); EXFOR-A1431 data file entry.
[53] S. Matsuki, S. Yamashita, K. Fukunaga, D. C. Nguyen, N. Fujiwara, and T. Yanabu, Jpn. Phys. J. **26**, 1344 (1969); EXFOR-A1435 data file entry.
[54] V. I. Chuev, V. V. Davidov, B. G. Novatsky, A. A. Oglobin, S. B. Sakuta, and D. N. Stepanov, J. Phys. (Paris), Colloq. **32**, C6–163 (1971).
[55] A. T. Rudchik, A. Budzanowski, E. I. Koshchy, L. Glowacka, Yu. G. Mashkarov, M. Makowska-Rzeszutko, V. M. Pirnak, R. Siudak, A. Szczurec, J. Turkiewicz, V. V. Uleshchenko, and V. A. Ziman, Nucl. Phys. **A602**, 211 (1996).
[56] S. N. Abramovich, B. Ya. Guzjovskij, B. M. Dzyuba, A. G. Zvenigorodkij, S. V. Trusillo, and G. N. Sleptsov, Bull. Russ. Acad. Sci. Phys. **40**, 129 (1976); EXFOR-A0117 data file entry.
[57] R. J. Slobodrian, Phys. Rev. C **125**, 1003 (1962).
[58] A. Auce, R. F. Carlson, A. J. Cox, A. Ingemarsson, R. Johansson, P. U. Renberg, O. Sundberg, and G. Tibell, Phys. Rev. C **53**, 2919 (1996).
[59] S. Mayo, W. Schimmerling, and M. J. Sametband, Nucl. Phys. **62**, 393 (1965).